REVIEW ARTICLE

Harnessing brain waves: a review of brain magnetic resonance elastography for clinicians and scientists entering the field

[1]ARVIN ARANI, PhD, [2]ARMANDO MANDUCA, PhD, [1]RICHARD L EHMAN, MD and [1]JOHN HUSTON III, MD

[1]Department of Radiology, Mayo Clinic, Rochester, MN, USA
[2]Physiology and Biomedical Engineering, Mayo Clinic, Rochester, MN, USA

Address correspondence to: Dr Arvin Arani
E-mail: *arani.arvin@mayo.edu*

ABSTRACT

Brain magnetic resonance elastography (MRE) is an imaging technique capable of accurately and non-invasively measuring the mechanical properties of the living human brain. Recent studies have shown that MRE has potential to provide clinically useful information in patients with intracranial tumors, demyelinating disease, neurodegenerative disease, elevated intracranial pressure, and altered functional states. The objectives of this review are: (1) to give a general overview of the types of measurements that have been obtained with brain MRE in patient populations, (2) to survey the tools currently being used to make these measurements possible, and (3) to highlight brain MRE-based quantitative biomarkers that have the highest potential of being adopted into clinical use within the next 5 to 10 years. The specifics of MRE methodology strategies are described, from wave generation to material parameter estimations. The potential clinical role of MRE for characterizing and planning surgical resection of intracranial tumors and assessing diffuse changes in brain stiffness resulting from diffuse neurological diseases and altered intracranial pressure are described. In addition, the emerging technique of functional MRE, the role of artificial intelligence in MRE, and promising applications of MRE in general neuroscience research are presented.

INTRODUCTION

Magnetic resonance elastography (MRE) is an MRI-based technology for quantitatively imaging the mechanical properties of tissues *in vivo*.[1] MRE is now widely used for the clinical evaluation of liver disease and is regarded as the most accurate non-invasive method for assessing liver fibrosis.[2,3] Ongoing research has indicated that MRE has potential applications in assessing other organ systems.[4–6] One of the most promising emerging applications is the use of MRE to non-invasively measure the mechanical properties of the living human brain. Some of the quantitative metrics that can be explored are storage modulus, loss modulus, viscosity, damping, non-linearity, dispersion, anisotropy, and the functional mechanics of the brain.[7] The measurement of the mechanical properties of the brain can then be used to investigate biological changes from the normative state to various disease states resulting from the formation of tumors, demyelination, increased/decreased intracranial pressure, or altered functional states.[8–10] This information can provide both global and localized estimates of quantitative mechanical properties of brain tissue, including regions that are inaccessible to palpation, and can act as a probe into tissue function. The mechanical properties of tissue are used to non-invasively measure the stiffness and viscosity of brain tissue. However, the complexity and inherent anisotropy of brain tissue, as well as common confounders such as brain atrophy, can impact the accuracy of these measurements. This review article has three objectives: (1) to give a general overview of the types of measurements that have been obtained with brain MRE in patient populations, (2) to help readers identify what tools are currently being used in the field in order to make these measurements possible, and (3) to highlight brain MRE applications that have the highest potential of being adopted into clinical use within the next 5 to 10 years. Applications of MRE for assessing brain disease are currently investigational and the studies discussed in this review were conducted with the approval of institutional review boards and written informed consent of the patients.

MAGNETIC RESONANCE ELASTOGRAPHY METHODOLOGY

MRE is composed of three steps: (i) actuation, (ii) imaging the vibrations, and (iii) generating images of the mechanical properties of tissue from the vibrational information.

Actuation - the generation of vibrations

The introduction of vibrational motion (more precisely, shear waves) into the brain is generally required for most applications of MRE. Many groups have investigated unique ways of generating vibrations into the brain including scanner table motion,[11] bite-bars,[12] and utilizing intrinsic pulsatile motion.[13] For a combination of reasons, such as limited wave amplitudes, long scan durations, and patient comfort, the two most commonly adopted approaches for human use have been: (i) a pneumatic active driver with a pillow-type passive driver[14] and (ii) a head-rocker unit in conjunction with a rigid rod.[15] Recently, McGrath et al[16] used simulations to test the optimal wave delivery methodology for brain MRE and concluded that the pillow and head-rocker approaches resulted in the lowest levels of errors in stiffness map inversions. MRE of the brain can be implemented using the standard active pneumatic driver equipment available in regulatory-approved commercial implementations of MRE, with the addition of a specially constructed pillow-like passive driver, as illustrated in Figure 1. As depicted, the active driver is located in the equipment room, outside the MRI scan room, and sends longitudinal (sound) waves through a flexible plastic tube to a passive pillow-like driver that is placed under the subject's head. The passive pillow driver transmits acoustic energy through the brain, a proportion of which is converted into shear waves, due to mode conversion. In human applications, where an external vibration source is used to achieve steady-state motion, frequencies between 20 and 150Hz have previously been used.[17-23] However, due to the increase in attenuation at higher frequencies and signal-to-noise considerations, frequencies in the range of 60Hz are used in the clinical research environment. Uffmann et al[24] provide a summary of several external actuation methods used for MRE. Alternatively, intrinsic activation techniques rely on measuring waves produced from a cardiac or pulsatile impulse function and converting that to brain stiffness/viscosity measurements.[13,25,26] The three-dimensional wave field that is generated by either the external or intrinsic vibrations is then encoded and captured with motion encoding MRI pulse sequences.

Motion encoding - imaging the vibrations

Once vibrations are propagating throughout the brain, a phase contrast MRI imaging sequence that is time-locked to the vibrational motion is used to encode the displacements into the phase of the MRI signal. Detailed descriptions of this phenomenon have been given in previous publications[1,27] and the gradients used are referred to as motion encoding gradients (MEGs). The wave information needs to be acquired in a stroboscopic fashion in order to capture the wave propagation at difference vibrational phases, commonly referred to as phase offsets. These phase-offsets are usually spaced evenly over the period of the vibrational motion by applying a time delay between the MEGs and the physical vibration. In addition, three directions of motion, as well as a single no-motion reference image, or two images at each offset (with opposite polarity) are commonly acquired to perform phase subtraction to suppress static phase variations from the vibration related phase accrual. The phase subtracted images are usually the input to wave inversion algorithms, which will be discussed in detail in the next section.

In a typical clinical research workflow, phase images are automatically subtracted and stiffness (elastograms) and viscosity maps may be generated on the scanner itself. The collection of phase difference images across all vibrational phase offsets and in all physical motion encoding directions gives the full 3D displacement field at each phase offset.

In clinical research studies, where full brain coverage is desired, brain MRE is often done using echo-planar-imaging (EPI) sequences (both spin-echo, or gradient echo) due primarily to short acquisition times and on-scanner reconstruction capabilities.[23,28] Some studies have used spiral acquisition strategies[29,30] to give fast high-resolution acquisitions. MRE acquisition pulse sequences are an active area of research and many new strategies to improve scanning efficiency and resolution have been proposed. A number of groups are working on increasing the efficiency of traversing the large MRE parameter space using

Figure 1. Experimental setup of brain MRE using a pneumatic driver. With MR Elastography, an active pneumatic mechanical wave driver is located outside the MRI scan room. The active pneumatic driver is connected by a flexible plastic tube to a passive pillow driver placed under the head. The passive pillow driver generates continuous acoustic vibration that is transmitted through the entire brain at a set vibration frequency (60Hz in this example).
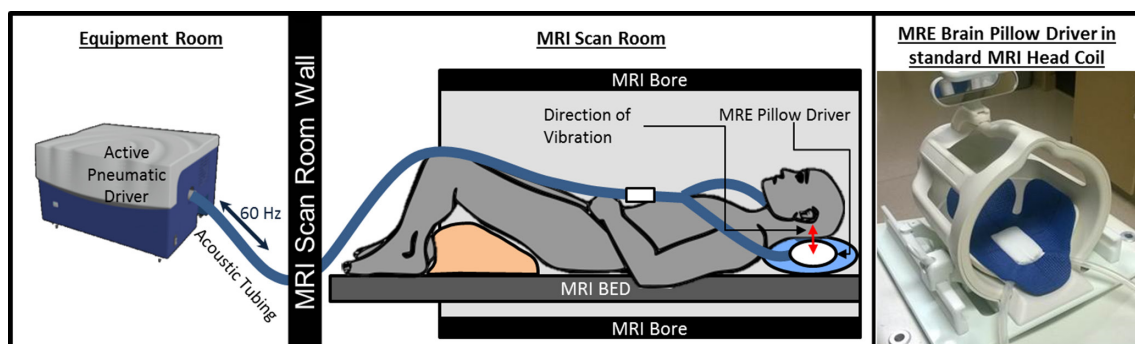
Table 1. MRE metrics

Primarily tissue stiffness-related metric	Primarily viscosity-related metric
Storage modulus (G')	Loss modulus (G")
Relative/ratio measures of stiffness and viscosity	Combination of elasticity and viscosity
Damping ratio/Fluidity Lost tangent/Phase angle	Magnitude of shear modulus ($\|G^*\| = \|G'+iG"\|$) Wave speed Shear stiffness (density*wave speed squared)

fractional encoding techniques,[31] sample-interval modulation (SLIM-MRE),[32,33] reduced field of view,[34] simultaneous multi-slice/multi-band acquisitions,[35,36] and true 3D MRI acquisition[37] schemes to boost performance. All of these techniques require specialized MRI acquisition sequences and post processing techniques that have been developed by investigators in the field and shared with collaborators, but are not yet available commercially.

Elastograms – generating images of tissue mechanics

Once the 3D displacement fields are imaged, the information from the displacement data is used to extract quantitative mechanical properties of the underlying tissue. Metrics used to describe the stiffness and viscosity of tissue in the MRE literature are outlined in Table 1. Strategies for relating metrics between studies have been described by Hiscox et al[7].

The conversion from displacement data to a map of any of the tissue properties described in Table 1 relies on mathematical algorithms collectively referred to as inversion algorithms. Several classes of algorithms exist, and it is important to choose an appropriate one for a given application. Inversion algorithms for MRE have been the focus of several reviews.[38,39]

It should be noted that the displacement data that is acquired is usually composed of longitudinal waves and shear waves, both at the driving frequency and at higher harmonics. In brain MRE, shear waves at the fundamental/driving frequency are the primary signal being investigated. Generally, a temporal Fourier transform is used to extract motion at the vibrational driving frequency to help eliminate the contributions of higher harmonic motion. However, this will not remove longitudinal waves, since they are also vibrating at this frequency. Therefore, accounting for the impact of longitudinal waves is of utmost importance for brain MRE. This can either be done by taking the curl of the displacement field,[40] or by accounting for longitudinal waves in the underlying inversion algorithms. Since longitudinal waves have extremely long wavelengths/wave speeds (~1400 m/s *vs* 1–10 m s^{-1} for shear waves), not accounting for them can result in significantly biased results.

Two types of inversion algorithms commonly used for brain MRE are variations of direct inversion (DI)[39,41–43] and non-linear inversion (NLI).[44,45] Both DI and NLI give an estimate of the complex shear modulus (G'+iG"), giving maps of both tissue

stiffness and viscosity. In the DI algorithm, local homogeneity is assumed (*i.e.* the material properties are assumed to not change within a small local neighborhood). This simplifies the equation of motion, reducing it to the Helmholtz equation, which is then solved. One of the earliest implementations was described in 2001 by Oliphant et al, who used a least squares estimation with the following cost function[41]:

$$\hat{\mu} = \arg\min_{\mu} \left\| \nabla^2 \vec{u} \cdot \mu + \rho\omega^2 \vec{u} \right\|_2^2 = -\rho\omega^2 \left[\nabla^2 \vec{u} \right] \vec{u}$$

where μ is the shear modulus, *u* is the 3-dimensional (3 × 1) displacement vector (or curl of the displacement vector) of a single voxel, ρ is the density, ω is the angular velocity, ∇^2 is the 3D Laplace operator, and † is the pseudo inverse. The advantage of this approach is that even with full 3D brain volume data sets, it is fast enough to be reconstructed on the scanner while the subject is still on the table. An example of an MRE SE-EPI pulse sequence including the output curled displacements fields in all three motion encoding directions, a T1W image, and a DI elastogram at the same slice location, are shown in Figure 2.

NLI uses a finite element model (FEM) to solve the forward wave equation. It then uses overlapping subzones of the acquired displacement field to iteratively solve the inverse problem by minimizing the error between the FEM forward model and the acquired displacement field. The subzones are combined to make a full stiffness map. Soft prior regularization is sometimes applied to encourage similar material property values within a specific anatomic region.[45] This approach takes hours to converge, but has the advantage of relaxing the homogeneity assumption commonly used in the DI algorithm. Both DI and NLI assume that the tissue is isotropic in its material properties.

Anisotropic inversions take tissue fiber orientation into account. In muscles, shear waves propagate significantly more quickly along the fiber direction than they do perpendicular to the fiber.[46–49] This is thought to also occur to some extent in brain white matter fibers, and evidence supporting this theory was shown by Anderson et al[50] when they applied vibrational energy in different directions and observed changes in stiffness estimates. Romano et al[51] have developed an anisotropic MRE inversion algorithm that uses directions obtained from diffusion tensor imaging (DTI) fiber tractography measurements to obtain stiffness measurements perpendicular and parallel to the fiber tracts. In 14 patients with Amyotrophic Lateral Sclerosis (ALS), parallel and perpendicular stiffness estimates were significantly lower in ALS patients than in 14 normal age-matched healthy controls. Alternatively, Tweten et al[52,53] utilized directional filters and only MRE data to calculate anisotropic stiffness information and have validated their approach in simulations. An example of Tweten's simulation in incompressible, transversely isotropic (ITI) material is shown in Figure 3. Finally, Schmidt et al[54] measured anisotropic mechanical properties in *ex vivo* white matter in a porcine model. In a well-controlled experimental setup and a finite element inversion, they reported that the porcine brain only exhibited "mild" anisotropic behavior. More simulation, phantom, and *in vivo* validation are needed in this area to determine what impact brain anisotropy has on MRE

Figure 2. An example of a spin echo echo-planar-imaging MRE pulse sequence. Image Acquisition: the motion encoding gradient (MEG) can be applied on x-, y-, and z-gradient to detect the harmonic motion in each direction. The time delay between the motion and the MEGs is changed to obtain stroboscopic-types images of the steady-state wave pattern at different phases of propagation. RF – radiofrequency pulses, G(x,y,z) – gradient wave forms in each Cartesian direction, M – vibrational motion, SSP – spatial-spectral RF pulse, MEG – flow-compensated motion-encoding gradients, ET – EPI echo train. Post-processed output images: The top three images are the displacement fields in three spatial directions after the curl operator has been performed to remove any longitudinal components from the displacement field. A T1W image is shown for anatomical reference to the quantitative stiffness map (elastogram) of the same axial slice in the brain.
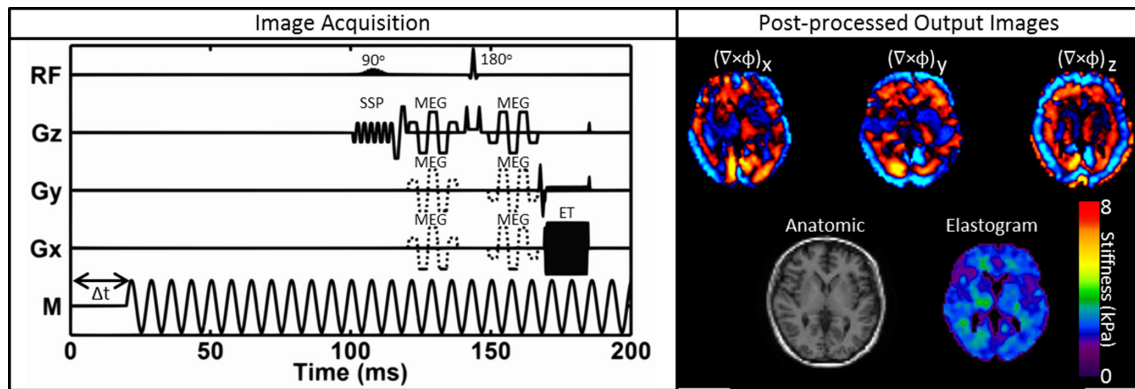
QUALITATIVE TUMOR STIFFNESS ASSESSMENT IN THE CLINIC

In the clinical research environment at our institution, brain MRE is primarily used for the qualitative visual assessment of preoperative intracranial tumors. Elastograms are obtained directly from the scanner and primarily viewed on workstations or in reading rooms by clinicians. Intracranial tumors are treated with surgery when the loss of severe neurological function can be spared. Surgical strategies vary depending on tumor consistencies; soft tumors generally require less invasive endoscopic and keyhole surgeries, while firm fibrotic tumors may require more open surgery strategies. Conventional MRI has shown some success in pre-operatively identifying extreme cases of extra axial tumor stiffness, very soft (high T2 signal) as opposed to very stiff (low T2 signal),[55] but grading stiffness quantitatively with standard MRI sequences is not currently possible. For this reason, one of the first clinical applications of brain MRE will most likely be pre-surgical planning for tumor resection. Specifically, for the information it provides in terms of tumor stiffness as well as tumor adhesion to adjacent tissues.

Preoperative assessment of intracranial tumors

Overall, MRE stiffness has been shown to preoperatively agree with a surgeon's intraoperative assessment of intracranial tumor stiffness. The first comparative study showing agreement between surgical assessment and pre-operative MRE stiffness was conducted in 2007 by Xu et al[17]. They reported that despite a range of viscoelastic properties in these tumors (from soft to hard), all six MRE predictions agreed with surgical findings. Further support that MRE is able to predict surgical assessment was given in three studies from our institution[56–58]; two studies conducted in meningiomas (12 and 14 subjects) and one in pituitary adenomas (10 subjects). In 2016, Sakai et al[59] showed that intraoperative tumor consistency correlated with MRE findings in 34 tumors (13 meningiomas, 11 pituitary adenomas, six vestibular schwannomas, and four gliomas), as summarized in Figure 4. An example of pre-surgical MRI and MRE axial images, and corresponding surgical assessments in two patients with meningiomas have been shown in Figure 5.

The impact of brain MRE for pre-surgical assessment is anticipated to be quite high. However, as with any new diagnostic technology, care needs to be taken in understanding what artifacts and pitfalls are present in MRE stiffness maps. Image signal-to-noise, tissue inhomogeneity, edge effects, and large wavelengths in stiff tissues can impact the accuracy of stiffness estimates in tumors, making small tumors and/or heterogeneous tumors with high vascularity challenging to assess. Clinical adoption will require future studies with much larger sample sizes in order to understand the true impact of this technique.

Assessment of tumor adherence

Tumor adhesion to normal brain tissue also has a direct impact on the difficulty of tumor resection. An MRE displacement field can also be used to generate a qualitative measure of tumor adhesion, referred to as slip interface imaging (SII).[60] SII uses discontinuities in the displacement field to probe tissue/tumor boundaries that are slipping relative to one another as wave energy is transferred between two mediums. These slips result in relatively high spatial gradients in displacement that can be detected as high strain values in normalized octahedral strain (OSS) images. Yin et al have shown the clinical utility of SII imaging in meningiomas[61] and vestibular schwannomas,[60] reporting a high degree of correlation with intraoperative assessment of tumor adherence. An example of SII images in a patient with a meningioma is shown in Figure 6. Some non-slip factors such as quick changes in wavelength due to large modulus contrasts, as well as wave scattering at interfaces, can impact these measurements and need to be considered during pre-surgical planning.[62,63]

Figure 3. Approach for creating analytical slow and fast shear wave data sets in three propagation directions. (a) Analytical data sets were created in a $70 \times 70 \times 70\,mm^3$ cube of ITI material with a voxel size of $1\,mm^3$; a fiber direction of $\alpha = [1/\sqrt{2}, 0,-1/\sqrt{2},]$; and material properties of $\mu = 1000$ Pa, $\phi = 1$, $\zeta = 2$, and $\eta = 0.2$. The displacements of the slow and fast shear waves relative to their polarizations are shown in (b) and (c), respectively. The polarizations of the slow m_s and fast m_f shear waves are shown with respect to the propagation directions $n_1 = [\sin15°; 0; -\cos15°]$ (d), $n_2 = [0; \sin1°; -\cos1°]$ (e), and $n_3 = [\sin15°; 0; -\cos15°]$ (f). Relative displacements of the slow and fast shear waves are compared for the propagation directions n_1 (g), n_2 (h), and n_3 (i). Slow shear wave displacements are displayed in the white planes in (d), (e), and (f), and the fast shear wave displacements are shown in the planes which include the fiber directions (black stripes). (From Tweten DJ., et al. Requirements for accurate estimation of anisotropic material parameters by MRE: a computational study. Magnetic resonance in medicine, 78(6), pp.2360–2372. Reproduced with permission from John Wiley and Sons).
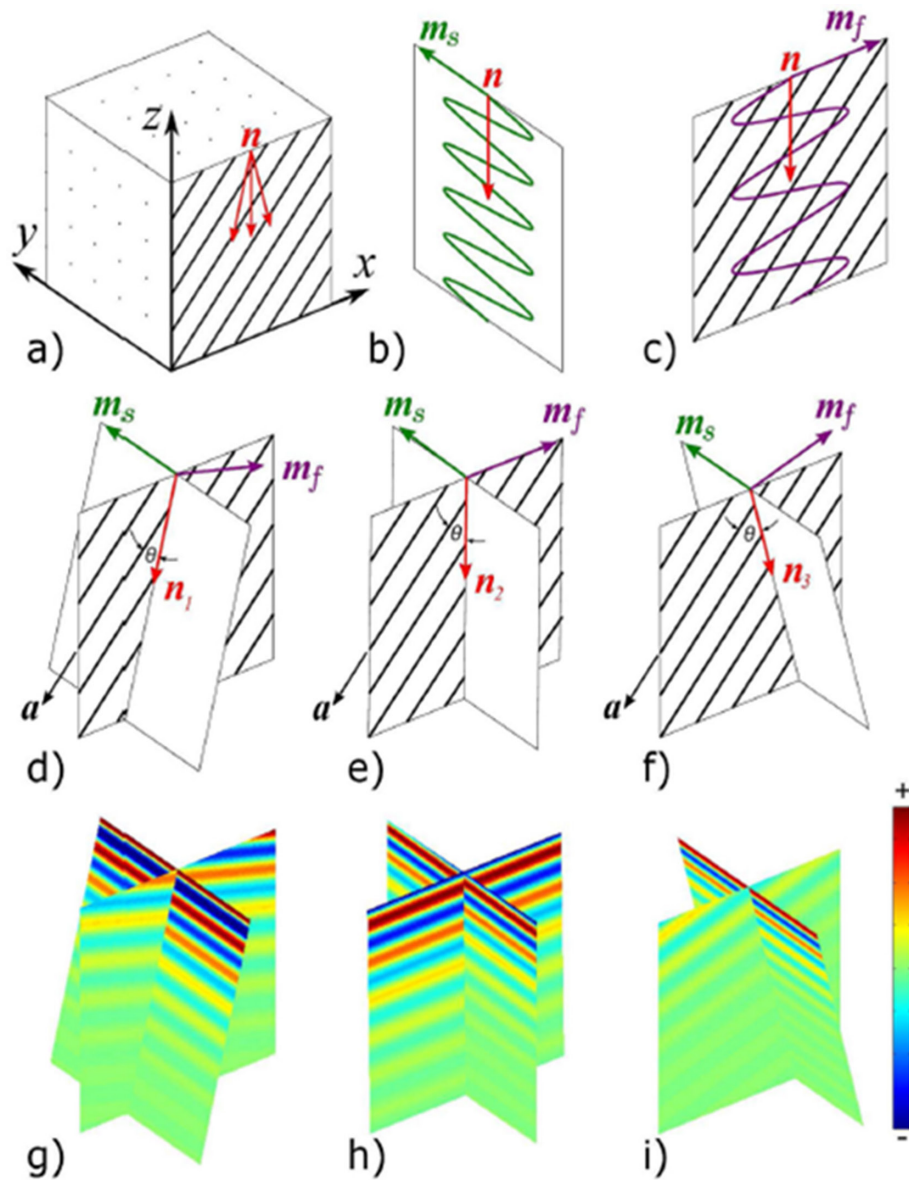
## QUANTITATIVE ASSESSMENT OF BRAIN TISSUE WITH MRE

The quantitative assessment of brain tissue using MRE is an active area of research that, to date, has had two areas of focus; (1) intra axial tumor differentiation and grading, and (2) understanding the diffuse mechanics of brain tissue. The former has primarily been instructive for diagnostics and prognostics, while the latter is likely to provide important insights into the mechanisms and pathophysiology of both disease and normative changes with aging.

Tumor differentiation and grading

The ability of MRE to quantitatively measure the mechanical properties of brain tissue, *in vivo,* has motivated several investigations into its potential for intra axial tumor differentiation and grading. In 2013, Streitberger et al[64] showed that glioblastomas

Figure 4. Scatterplot of the meanSS and maxSS (kPa) determined by using an MRE and a 5-point scale of intraoperative qualitative assessment of tumor consistency in 34 patients with four common intracranial tumors. Both the $_{mean}$SS and $_{max}$SS were significantly correlated with the surgeon's grading p <.05) (Spearman rank order test). (From Sakai N., et al. Shear stiffness of four common intracranial tumors measured using MR elastography: comparison with intraoperative consistency grading. Am J Neuroradiol. 2016;37(10):1851–59. Reproduced with permission from American journal of neuroradiology).
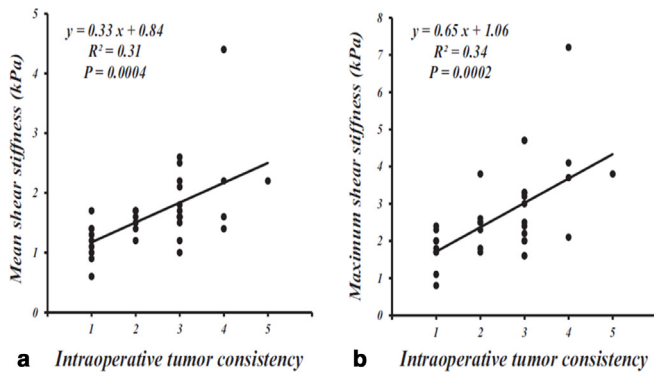
were softer than healthy brain parenchyma. Simon et al[65] corroborated this finding by qualitatively comparing three glioblastomas with the contralateral parenchymal stiffness and showed a range of mechanical properties between different tumor types (Figure 7). Pepin et al[66] demonstrated in 18 subjects that glioblastomas were not only softer than brain parenchyma, but that grade IV gliomas were significantly softer than grade II gliomas. This study also reported that gliomas with isocitrate dehydrogenase 1 (IDH1) gene mutations were stiffer than IDH1-wild type gliomas. Although gliomas were shown to be universally softer than brain parenchyma, other tumor types were heterogeneous and had regions that were both soft and hard. Reiss-Zimmermann et al[67] also showed this to be true, but reported that they could clearly differentiate meningiomas from four other tumor types (glioblastoma, anaplastic astrocytomas, cerebral metastasis, and intracerebral abscesses). Understanding the mechanisms behind these mechanical changes, as well as large-scale clinical research studies will be needed prior to clinical use. Brain tumor assessment with MRE has been reviewed in.[68,69]

Diffuse disease and brain biomechanics
Investigation into non-localized or diffuse brain biomechanics is another application for MRE. This generally involves neuroimaging, post-processing, and MRE inversion expertise in order to fit atlas segmentations from T1W images to the MRE data and to help compensate for edge and partial volume/CSF contamination effects. As a result, these measurements have only been demonstrated in research settings and not in standard clinical research workflow. Nevertheless, there has been a large amount of work done to understand the correlations of global and regional MRE stiffness measurements in healthy and diffuse disease.

The test-retest repeatability of brain MRE has been evaluated for echo-planar and spiral acquisition strategies using direct

inversion and non-linear inversion, respectively. A test re-test repeatability study in 10 healthy subjects, using a 3 mm isotropic imaging resolution, and a DI type algorithm[39] reported errors of less than 1% for global median measurements and less than 2% for regional median measurements.[20] In a similar study on one volunteer, Johnson et al[70] reported errors of 3–7% in subcortical grey matter regions using a 1.6 mm isotropic resolution MRE scan and an NLI[45] algorithm to estimate stiffness. Huang et al[71] reported a within subject coefficient of variation of 1.8–6.0% in white matter, gray matter and whole-brain shear stiffness measurements for vibration frequencies of 40 Hz, 50 Hz, and 60 Hz. These results demonstrate the high reproducibility of brain MRE in healthy human subjects with errors ranging from 1 to 7%.

In the healthy adult brain, there is a general consensus that the cerebrum becomes less stiff as we age.[72,73] However, this trend may not be consistent throughout the aging process. A study in 46 adolescent subjects (12–14 years old) showed no significant difference in global brain stiffness when compared to a cohort of twenty 18–33-year-olds.[74] However, stiffness values in the cerebellum, parietal, and temporal lobes were found to be significantly different between the two cohorts. In adults, there is also some evidence that sexual dimorphism exists[72,75] with females being stiffer in some brain regions, but there have also been studies that have shown no significant sexual dimorphism in aging adults, or in the transitional period from adolescence to adulthood.[74,76] Different methodologies, regional dependencies, and patient cohorts may contribute to these differences, but further work is needed to come to a consensus.

The topography of the stiffness of the brain is still under investigation. There is general agreement that the cerebrum is stiffer than the cerebellum.[20,30,77] Deep gray nuclei have been reported to be stiffer than surrounding white matter, which agrees with a report that cortical gray matter is stiffer than white matter.[18] However, much of the field reports that white matter is stiffer than cortical gray matter.[12,22,77–81] The combination of cerebral spinal fluid, partial volume effects due to large voxel sizes, and the relatively thin gray matter ribbon, makes measuring the stiffness of cortical gray matter challenging and may contribute to these discrepancies. In addition, agreement has not been reached amongst different research groups as to what inversion algorithms, image parameters, segmentation approaches, or even acquisition methods are best suited to overcome these challenges, leaving the development of a stiffness atlas for the brain an active area of research with a need for standardization. Recently, Hiscox et al[82] have published an effort to establish a standard-space atlas of the viscoelastic properties of the human brain and have made their templates openly available at (github.com/mechneurolab/mre134) to help foster collaborations across research institutions.

The first brain MRE investigation showing that global stiffness could be an indicator of pathology was conducted in patients with multiple sclerosis (MS) by Wuerfel et al[75]. The study showed that patients with MS had a 13% (p < 0.001) decrease in cerebral viscoelasticity when compared to age and gender matched

Figure 5. Axial T1-weighted images(a, c) and their corresponding elastograms (b, d) for two meningiomas with different mechanical properties. For the case in the top row, the surgical report stated that the tumor was firm laterally and soft around the brain stem, which corresponds nicely with the stiffness map. For the case in the bottom row, the surgeon reported a mixture of very firm and somewhat medium stiffness, which is also apparent in the corresponding elastogram. These examples demonstrate the clinical potential of using MRE for pre-surgical assessment. The elastograms were generated using a DI inversion, and a post-processing pipeline that can be implemented directly on the scanner itself. (This study was approved by our institutional review board and the subjects gave written informed consent.)
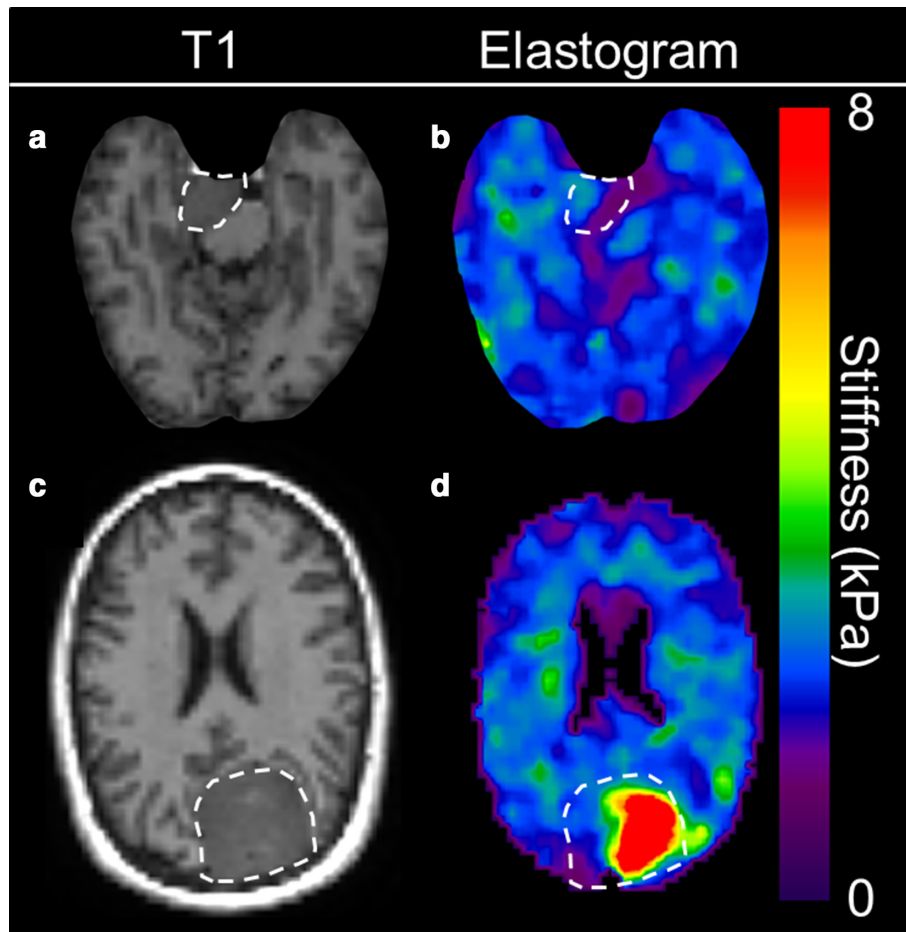

healthy controls. Subsequently, Steitberger et al[83] demonstrated, with a multi-frequency approach, that the chronic-progressive disease course caused significant alterations in wave dispersion, while the relapsing-remitting form did not. This suggests brain MRE could potentially be prognostic for MS. Brain MRE was extended to be evaluated as a biomarker for dementia by Murphy et al[84], who demonstrated that there was a reduction in global brain stiffness in patients with Alzheimer's disease (AD). Stiffness changes over the four most common causes of dementia (AD, dementia with Lewy bodies, frontal temporal dementia, and normal pressure hydrocephalus (NPH)) versus age-matched controls, has been summarized by ElSheikh et al[85]. The four forms of dementia exhibited unique patters of stiffness suggesting that MRE could be used as a potential differentiating biomarker. Lipp et al[86] have also shown a decrease in brain stiffness due to both Parkinson's disease and progressive supranuclear palsy (PSP), and suggested that mesencephalic stiffness can be used to discriminate PD from PSP. This body of work strongly supports the theory that demyelination and neurodegeneration result in the softening of the brain, often with specific topography.

The impact of intracranial pressure (ICP) on brain stiffness is another active area of research since homeostasis of ICP is of paramount importance to normal brain function. Groups have found significant correlations between acute changes in stiffness and pressure, venous drainage (Figure 8), hypercapnia, and perfusion.[87–90] However, the technique has been less sensitive to measuring changes due to less acute effects such as lumbar punctures.[91] There are also conflicting reports related to the effect of NPH on brain stiffness. Some studies have shown that global stiffness decreases due to NPH,[92,93] while other studies have observed localized increases in brain stiffness.[94–96] Recently, Murphy et al[97] in a cohort of 85 participants (44 cognitively unimpaired, 33 with NPH, and eight amyloid positive with Alzheimer clinical syndrome), used a customized neural network inversion to enable a voxel-wise analysis to help visualize unique patterns of

Figure 6. Concordant case with a partial slip interface at imaging and partial adhesion at surgery (case 17, 49-year-old female). (a) Sagittal T1W image with contrast enhancement shows a petroclival meningioma. The tumor–brain interface is partially defined in the (b) shear line image, (c) OSS map, and (d) normalized OSS map with arrows indicating the presence of a slip interface and arrowheads indicating the absence of a slip interface, suggesting the tumor was partially adherent to the brainstem. At surgery, the dissection plane was also classified as mixed adhesion, corresponding to the SII findings. (From Yin Z, et al. Slip interface imaging based on MR-elastography preoperatively predicts meningioma–brain adhesion. J Magn Reson Imaging 2017;46(4):1007–1016. Reproduced with permission from John Wiley and Sons).
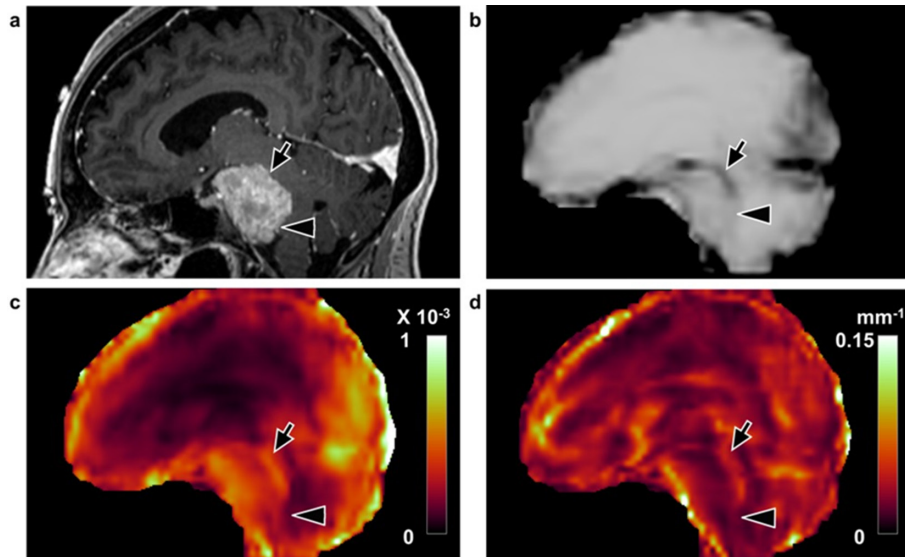
viscoelastic alterations due to NPH. Considering both damping ratio and stiffness estimates, they devised an NPH score for each participant and reported an area under the receiver operator characteristic curve of 0.999 and 1 for separating an NPH cohort from cognitively unimpaired and amyloid-positive with Alzheimer clinical syndrome cohorts, respectively. Furthermore, they showed that NPH presented as a concentric pattern of stiffening near the dural surface at the vertex and softening near the ventricles, suggesting that different regions of interest could possibly explain the discrepancies previously reported in the field. Altogether, these promising results emphasize the potential and show the need for more work to be done in exploring the relationship between viscoelasticity and ICP.

While MRE is designed to be a quantitative technique, there are many limitations and simplifying assumptions that need to be kept in mind. For instance, measurements of stiffness in regions where stiffness varies over a small distance may be inaccurate due to limitations in the way that stiffness is calculated by the inversion algorithm. Most of the work reported in the sections above has been done with specialized post-processing pipelines and offline reconstructions tailored to the specific application. However, the choices and assumptions made in different studies have resulted in differences in MRE acquisition parameters, inversion algorithms, segmentation pipelines, and reported parameter estimates. These discrepancies have limited the ability to give direct quantitative comparisons between studies. Furthermore, the majority of the studies conducted in the field have limited sample sizes, making it challenging to accurately interpret the significance of many of these findings. Although methodological strategies introduce error and uncertainty, developments are underway to help improve accuracy and precision. Multi-center

studies and larger sample sizes, especially for applications like pre-surgical assessment that are likely to be adopted for clinical use in the near future, are required to propel brain MRE into clinical acceptance, in addition to technical improvements.

EMERGING AND FUTURE PERSPECTIVES

There are several cutting-edge techniques being explored that are pushing the limits of MRE for neuroimaging applications. Due to space limitations and existing reviews on many of these topics,[7–10,81] we will focus on two: (i) functional mechanics, and (ii) artificial intelligence. Development in these two technologies is likely to play a pivotal role in the future of brain MRE.

Functional mechanics

MRE is emerging as a new method for imaging the response of tissue viscoelasticity to functional processes. This is dual-faceted; some groups are looking at steady-state structure-function relationships in hopes of predicting cognitive function or a response to conditioning or learning, while others are investigating the acute response to stimulation or task-based responses. Schwarb et al[98] demonstrated in 20 young healthy adults that the hippocampal damping ratio was a significant predictor of relational memory task performance, while no relationship was observed with hippocampal volume. Differences in viscoelasticity as a result of aerobic fitness,[99] as a predictor of memory-task performance in older healthy adults,[100] and due to exercise training in MS patients[101] have also been shown to be significant. The first human study to show a correlation between an acute visual stimulus and stiffness was conducted in 57 volunteers by Fehlner et al[102]. They observed a 2.5% decrease in global brain stiffness, but did not see a localized effect in the visual cortex. Much of the later work, in localized regions, has reported an increase in

Figure 7. Anatomical scans and parameter maps of three cases with high similarity on conventional MRI: patient 11 presented with an anaplastic oligoastrocytoma (WHO III); patient 12 with a benign meningeoma (WHO I); and patient 16 with a high-grade glioblastoma (WHO IV). In contrast to the similarity on the anatomical conventional MRI, the biomechanical properties distinctly differentiate the tumor entities on the parameter maps, as already visible to the naked eye. ROI are demarcated as red dotted lines. (a) FLAIR; (b) T_1-weighted MRI, (c) MRE magnitude image contrast (T2*-weighted), (d) $|G^*|$-map and (e) and phase angle (ϕ) -map. (From Simon M, et al. Non-invasive characterization of intracranial tumors by MRE. New J. Phys. 2013;15 085024. Reproduced with permission from Institute of Physics Publishing under the terms of the Creative Commons Attribution 3.0 license).
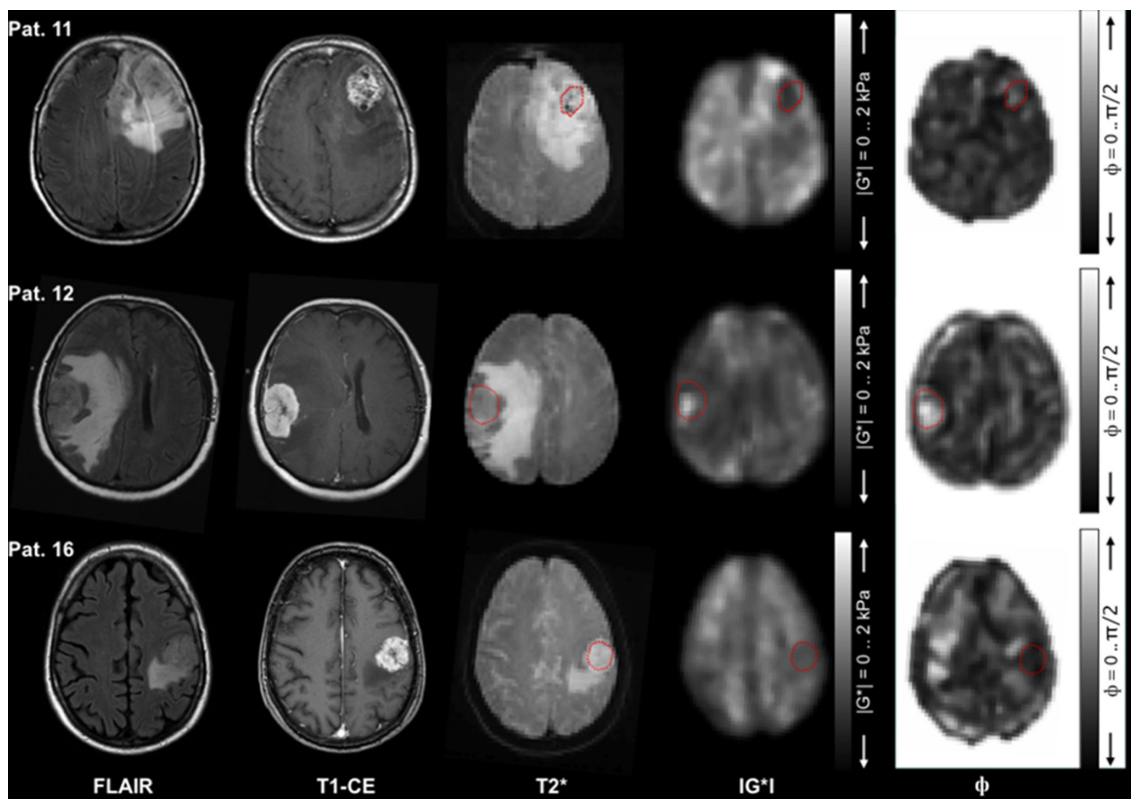

Figure 8. The relationship between shear moduli and the percentage of jugular vein flow with the cervical wrap in place. Storage modulus (G', left) and loss modulus (G'', right). Error bars are standard error of the mean in both panels. Both storage and loss moduli are significantly correlated with the percentage of jugular vein flow with the cervical wrap in place (*P*.05). (From Hatt A., et al. MR Elastography Can Be Used to Measure Brain Stiffness Changes as a Result of Altered Cranial Venous Drainage During Jugular Compression. American Journal of Neuroradiology 36.10 (2015): 1971–1977. Reproduced with permission from American journal of neuroradiology.).
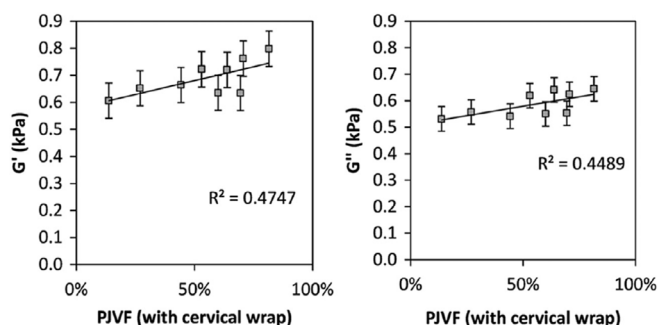

stiffness due to stimulation. Patz et al[103,104] and De Arcos et al[105], reported 10–20% increases in group-wise localized stiffness in both mice and humans. Lastly, in eleven subjects, Lan et al[106] used a time series analysis similar to Fehlner et al[102], and were able to show a significant 6–11% (mean: 7.57±1.31%) increase in stiffness localized to the visual cortex on a subject level. They used the magnitude information from this same data to simultaneously calculate traditional functional MRI activation maps, which only demonstrated a 1–2% signal range across subjects, but showed similar activation patterns (Figure 9). This body of work strongly suggests a correlation between brain viscoelasticity and function and offers a completely new and independent mechanism for exploring tissue function. Currently, these measurements are only possible in a research setting. Bringing these types of exploration into the clinical research environment should be a significant focus of future endeavors.

Artificial intelligence and MRE

The introduction of artificial intelligence (AI) in MRE postprocessing may help bridge the gap between research and clinical practice for current and future technically advanced MRE applications. AI could not only enable both online segmentations, using established brain atlases,[107] but could also be used to learn advanced MRE inversion algorithms. On-scanner segmentations

Figure 9. fMRE and fMRI *t*-score activation maps (*p* < 0.001) of the visual cortex for all 11 subjects; (top) stiffness-fMRE activation; (middle) BOLD-fMRI activation; (bottom) both fMRE (orange-yellow) and fMRI (blue-green) activation maps overlaid. (*From Lan PS, et al*. Imaging brain function with simultaneous BOLD and viscoelasticity contrast: fMRI/fMRE.[106]:11 6592. Reproduced with permission from Elsevier under a Creative Commons CC-BY-NC-ND License).
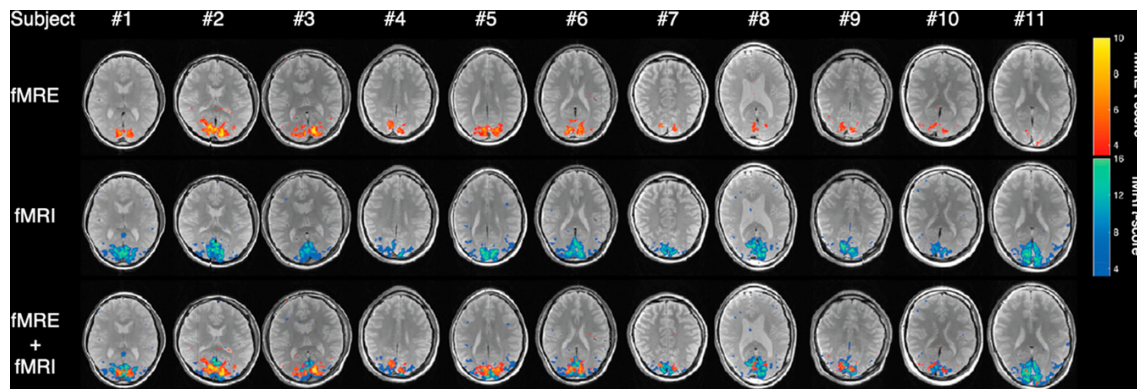
would enable localized stiffness estimates to be directly output from the scanner[108] and could potentially assist existing inversion algorithms to compensate for CSF contamination and edge effects.

Advanced inversion algorithms capable of relaxing the tissue homogeneity and/or isotropic elasticity assumptions, while maintaining adequate efficiency to be implemented in a clinically feasible timeframe, would help improve the accuracy of the technique in a clinical setting. Artificial neural networks trained on realistic constitutive equations of motion could help facilitate this transition into the clinic. Murphy et al[97,109] have recently developed a neural network inversion (NNI) that was more robust to noise than DI, while not only maintaining but also increasing measured biological effect sizes already established in both the liver and brain. Solamen et al[110] developed a convolutional NNI architecture and demonstrated feasibility in the brain. Scott et al[111] further relaxed the homogeneity assumptions initially made by,[97,109] and in simulation experiments they demonstrated an improvement in accuracy for predicting the stiffness of inclusions (≤2.25 cm in diameter) in no-noise, low-noise, and high-noise data, as compared to both DI and a homogeneous NNI, as well as sharper stiffness transitions at the edges of tumors. The inversion times for these techniques are generally within a clinically feasible timeframe suggesting potential to make research applications more accessible to clinical workflows. These results also motivate future work exploring the use of more advanced forward models for generating training data that are more representative of brain tissue mechanical behavior, such as existing viscoelastic,[112] and poroelastic models.[113]

CONCLUSIONS

Brain MRE is a powerful tool that can be used to provide valuable information to clinicians and researchers investigating the biomechanical properties of the brain. The application of brain MRE to assist in pre-surgical assessment is currently the most likely to be adopted into future clinical workflow, but the applications for research are ever expanding, and could offer great insights into many different disease processes. Larger sample sizes are needed for many of the applications covered in this review, and no large-scale multi-center brain MRE study has been conducted to date. Biological factors such as demyelination, neuronal cell body composition, dendrite composition, axonal density, axon size, cell packing density, complex microstructural interactions in the extracellular matrix, and intracranial pressure have all been suggested as contributors to measurable changes in stiffness and viscosity observed by MRE in different disease processes. If the key contributors can be identified, and direct causal relationships can be established between stiffness and pathology, this could lead to identifying and monitoring the early onset and progression of many neurological diseases in the future.

CONFLICTS OF INTEREST

Some of the authors and Mayo Clinic have a financial conflict of interest related to research funded by this grant.

REFERENCES

1. Muthupillai R, Lomas D, Rossman P, Greenleaf J, Manduca A, Ehman R. Magnetic resonance elastography by direct visualization of propagating acoustic strain waves. *Science* 1995; **269**: 1854–7. doi: https://doi.org/10.1126/science.7569924

2. Horowitz JM, Kamel IR, Arif-Tiwari H, Asrani SK, Hindman NM, et al. ACR appropriateness criteria® chronic Liver disease. *J Am Coll Radiol* 2017; **14**(11, Supplement): S391–405. doi: https://doi.org/10.1016/j.jacr.2017.08.045

3. Chalasani N, Younossi Z, Lavine JE, Charlton M, Cusi K, Rinella M, et al.

The diagnosis and management of nonalcoholic fatty liver disease: practice guidance from the American association for the study of liver diseases. *Hepatology* 2018; **67**: 328–57. doi: https://doi.org/10.1002/hep.29367

4. Low G, Kruse SA, Lomas DJ. General review of magnetic resonance elastography. *World J Radiol* 2016; **8**: 59–72. doi: https://doi.org/10.4329/wjr.v8.i1.59

5. Mariappan YK, Glaser KJ, Ehman RL. Magnetic resonance elastography: a review. *Clinical Anatomy* 2010; **23**: 497–511. doi: https://doi.org/10.1002/ca.21006

6. Glaser KJ, Manduca A, Ehman RL. Review of MR elastography applications and recent developments. *J Magn Reson Imaging* 2012; **36**: 757–74. doi: https://doi.org/10.1002/jmri.23597

7. Hiscox LV, Johnson CL, Barnhill E, McGarry MDJ, Huston J, van Beek EJR, et al. Magnetic resonance elastography (MRE) of the human brain: technique, findings and clinical applications. *Phys Med Biol* 2016; **61**: R401–37. doi: https://doi.org/10.1088/0031-9155/61/24/R401

8. Murphy MC, Huston J, Ehman RL. MR elastography of the brain and its application in neurological diseases. *Neuroimage* 2019; **187**: 176–83. doi: https://doi.org/10.1016/j.neuroimage.2017.10.008

9. Yin Z, Romano AJ, Manduca A, Ehman RL, Stiffness HJI. And beyond: what MR elastography can tell us about brain structure and function under physiologic and pathologic conditions. *Topics in Magnetic Resonance Imaging* 2018; **27**: 305–18.

10. Di Ieva A, Grizzi F, Rognone E, Tse ZTH, Parittotokkaporn T, Rodriguez y Baena F, ZTH T, y Baena FR, et al. Magnetic resonance elastography: a general overview of its current and future applications in brain imaging. *Neurosurg Rev* 2010; **33**: 137–45. doi: https://doi.org/10.1007/s10143-010-0249-6

11. Gallichan D, Robson MD, Bartsch A, Miller KL. TREMR: table-resonance elastography with Mr. *Magn Reson Med* 2009; **62**: 815–21. doi: https://doi.org/10.1002/mrm.22046

12. Uffmann K, Maderwald S, De Greiff A, Ladd M. Determination of gray and white matter elasticity with MR elastography. *Int Soc Magn Reson Med* 2004; **11**: 1768.

13. Weaver JB, Pattison AJ, McGarry MD, Perreard IM, Swienckowski JG, Eskey CJ, et al. Brain mechanical property measurement using MRE with intrinsic activation. *Phys Med Biol* 2012; **57**: 7275–87. doi: https://doi.org/10.1088/0031-9155/57/22/7275

14. Murphy MC, Huston J, Jack CR, Glaser KJ, Manduca A, Felmlee JP, et al. Decreased brain stiffness in Alzheimer's disease determined by magnetic resonance elastography. *J Magn Reson Imaging* 2011; **34**: 494–8. doi: https://doi.org/10.1002/jmri.22707

15. Sack I, Beierbach B, Hamhaber U, Klatt D, Braun J. Non-Invasive measurement of brain viscoelasticity using magnetic resonance elastography. *NMR Biomed* 2008; **21**: 265–71. doi: https://doi.org/10.1002/nbm.1189

16. McGrath DM, Ravikumar N, Beltrachini L, Wilkinson ID, Frangi AF, Taylor ZA. Evaluation of wave delivery methodology for brain MRE: insights from computational simulations. *Magn Reson Med* 2017; **78**: 341–56. doi: https://doi.org/10.1002/mrm.26333

17. Xu L, Lin Y, Han JC, Xi ZN, Shen H, Gao PY. Magnetic resonance elastography of brain tumors: preliminary results. *Acta radiol* 2007; **48**: 327–30. doi: https://doi.org/10.1080/02841850701199967

18. Green MA, Bilston LE, Sinkus R. *In vivo* brain viscoelastic properties measured by magnetic resonance elastography. *NMR Biomed* 2008; **21**: 755–64. doi: https://doi.org/10.1002/nbm.1254

19. Klatt D, Hamhaber U, Asbach P, Braun J, Sack I. Noninvasive assessment of the rheological behavior of human organs using multifrequency Mr elastography: a study of brain and liver viscoelasticity. *Phys Med Biol* 2007; **52**: 7281–94. doi: https://doi.org/10.1088/0031-9155/52/24/006

20. Murphy MC, Huston J, Jack CR, Glaser KJ, Senjem ML, Chen J, et al. Measuring the characteristic topography of brain stiffness with magnetic resonance elastography. *PLoS One* 2013; **8**: e81668. doi: https://doi.org/10.1371/journal.pone.0081668

21. Guo J, Hirsch S, Fehlner A, Papazoglou S, Scheel M, Braun J, et al. Towards an elastographic atlas of brain anatomy. *PLoS One* 2013; **8**: e71807. doi: https://doi.org/10.1371/journal.pone.0071807

22. Johnson CL, McGarry MDJ, Gharibans AA, Weaver JB, Paulsen KD, Wang H, et al. Local mechanical properties of white matter structures in the human brain. *Neuroimage* 2013; **79**: 145–52. doi: https://doi.org/10.1016/j.neuroimage.2013.04.089

23. Kruse S, Grimm R, Lake D, Manduca A, Ehman R. Fast epi based 3D MR elastography of the brain. *Proc Intl Mag Reson Med* 2006; **14**: 3385.

24. Uffmann K, Ladd ME. Actuation systems for MR elastography. *IEEE Eng Med Biol Mag* 2008; **27**: 28–34. doi: https://doi.org/10.1109/EMB.2007.910268

25. Hirsch S, Klatt D, Freimann F, Scheel M, Braun J, Sack I. In vivo measurement of volumetric strain in the human brain induced by arterial pulsation and harmonic waves. *Magn Reson Med* 2013; **70**: 671–83. doi: https://doi.org/10.1002/mrm.24499

26. Zorgani A, Souchon R, Dinh A-H, Chapelon J-Y, Ménager J-M, Lounis S, et al. Brain palpation from physiological vibrations using MRI. *Proc Natl Acad Sci U S A* 2015; **112**: 12917–21. doi: https://doi.org/10.1073/pnas.1509895112

27. Muthupillai R, Ehman RL. Magnetic resonance elastography. *Nat Med* 1996; **2**: 601–3. doi: https://doi.org/10.1038/nm0596-601

28. Hamhaber U, Sack I, Papazoglou S, Rump J, Klatt D, Braun J. Three-dimensional analysis of shear wave propagation observed by in vivo magnetic resonance elastography of the brain. *Acta Biomater* 2007; **3**: 127–37. doi: https://doi.org/10.1016/j.actbio.2006.08.007

29. Johnson CL, McGarry MDJ, Van Houten EEW, Weaver JB, Paulsen KD, Sutton BP, et al. Magnetic resonance elastography of the brain using multishot spiral readouts with self-navigated motion correction. *Magn Reson Med* 2013; **70**: 404–12. doi: https://doi.org/10.1002/mrm.24473

30. Johnson CL, Holtrop JL, McGarry MDJ, Weaver JB, Paulsen KD, Georgiadis JG, et al. 3D multislab, multishot acquisition for fast, whole-brain MR elastography with high signal-to-noise efficiency. *Magn Reson Med* 2014; **71**: 477–85. doi: https://doi.org/10.1002/mrm.25065

31. Rump J, Klatt D, Braun J, Warmuth C, Sack I. Fractional encoding of harmonic motions in Mr elastography. *Magn Reson Med* 2007; **57**: 388–95. doi: https://doi.org/10.1002/mrm.21152

32. Klatt D, Johnson CL, Magin RL, Simultaneous MRL. Simultaneous, multidirectional acquisition of displacement fields in magnetic resonance elastography of the in vivo human brain. *J Magn Reson Imaging* 2015; **42**: 297–304. doi: https://doi.org/10.1002/jmri.24806

33. Klatt D, Yasar TK, Royston TJ, Magin RL. Sample interval modulation for the simultaneous acquisition of displacement vector data in magnetic resonance elastography: theory and application. *Phys Med Biol* 2013; **58**: 8663–75. doi: https://doi.org/10.1088/0031-9155/58/24/8663

34. Sui Y, Arunachalam SP, Arani A, Trzasko JD, Young PM, Glockner JF, et al. Cardiac Mr elastography using reduced-FOV, single-shot, spin-echo epi. *Magn Reson Med* 2018; **80**: 231–8. doi: https://doi.org/10.1002/mrm.27029

35. Johnson CL, Sutton BP, Holtrop JL. Multiband, multishot magnetic resonance elastography. *Google Patents* 2020; **0**.

36. Majeed W, Kalra P, Kolipaka A. Simultaneous multislice rapid magnetic resonance elastography of the liver. *NMR Biomed* 2020; **33**: e4252. doi: https://doi.org/10.1002/nbm.4252

37. Sui Y, Arani A, Trzasko JD, Murphy MC, Rossman PJ, Glaser KJ, et al. TURBINE-MRE: a 3D hybrid radial-Cartesian epi acquisition for MR elastography. *Magn Reson Med* 2021; **85**: 945–52. doi: https://doi.org/10.1002/mrm.28445

38. Fovargue D, Nordsletten D, Sinkus R. Stiffness reconstruction methods for Mr elastography. *NMR Biomed* 2018; **31**: e3935. doi: https://doi.org/10.1002/nbm.3935

39. Manduca A, Oliphant TE, Dresner MA, Mahowald JL, Kruse SA, Amromin E, et al. Magnetic resonance elastography: non-invasive mapping of tissue elasticity. *Med Image Anal* 2001; **5**: 237–54. doi: https://doi.org/10.1016/S1361-8415(00)00039-6

40. Baghani A, Salcudean S, Rohling R. Theoretical limitations of the elastic wave equation inversion for tissue elastography. *J Acoust Soc Am* 2009; **126**: 1541–51. doi: https://doi.org/10.1121/1.3180495

41. Oliphant TE, Manduca A, Ehman RL, Greenleaf JF. Complex-valued stiffness reconstruction for magnetic resonance elastography by algebraic inversion of the differential equation. *Magn Reson Med* 2001; **45**: 299–310. doi: https://doi.org/10.1002/1522-2594(200102)45:2<299::AID-MRM1039>3.0.CO;2-O

42. Hirsch S, Guo J, Reiter R, Papazoglou S, Kroencke T, Braun J, et al. MR elastography of the liver and the spleen using a piezoelectric driver, single-shot wave-field acquisition, and multifrequency dual parameter reconstruction. *Magn Reson Med* 2014; **71**: 267–77. doi: https://doi.org/10.1002/mrm.24674

43. Papazoglou S, Hamhaber U, Braun J, Sack I. Algebraic helmholtz inversion in planar magnetic resonance elastography. *Phys Med Biol* 2008; **53**: 3147–58. doi: https://doi.org/10.1088/0031-9155/53/12/005

44. Van Houten EEW, Miga MI, Weaver JB, Kennedy FE, Paulsen KD. Three-dimensional subzone-based reconstruction algorithm for Mr elastography. *Magn. Reson. Med.* 2001; **45**: 827–37. doi: https://doi.org/10.1002/mrm.1111

45. McGarry M, Johnson CL, Sutton BP, Van Houten EE, Georgiadis JG, Weaver JB, et al. Including spatial information in nonlinear inversion Mr elastography using soft prior regularization. *IEEE Trans Med*

Imaging 2013; **32**: 1901–9. doi: https://doi.org/10.1109/TMI.2013.2268978

46. Kruse SA, Smith JA, Lawrence AJ, Dresner MA, Manduca A, Greenleaf JF, et al. Tissue characterization using magnetic resonance elastography: preliminary results*. *Phys Med Biol* 2000; **45**: 1579–90. doi: https://doi.org/10.1088/0031-9155/45/6/313

47. Gennisson J-L, Deffieux T, Macé E, Montaldo G, Fink M, Tanter M. Viscoelastic and anisotropic mechanical properties of in vivo muscle tissue assessed by supersonic shear imaging. *Ultrasound Med Biol* 2010; **36**: 789–801. doi: https://doi.org/10.1016/j.ultrasmedbio.2010.02.013

48. Gennisson J-L, Catheline S, Chaffaï S, Fink M. Transient elastography in anisotropic medium: application to the measurement of slow and fast shear wave speeds in muscles. *J Acoust Soc Am* 2003; **114**: 536–41. doi: https://doi.org/10.1121/1.1579008

49. Papazoglou S, Rump J, Braun J, Sack I. Shear wave group velocity inversion in MR elastography of human skeletal muscle. *Magn Reson Med* 2006; **56**: 489–97. doi: https://doi.org/10.1002/mrm.20993

50. Anderson AT, Van Houten EEW, McGarry MDJ, Paulsen KD, Holtrop JL, Sutton BP, et al. Observation of direction-dependent mechanical properties in the human brain with multi-excitation Mr elastography. *J Mech Behav Biomed Mater* 2016; **59**: 538–46. doi: https://doi.org/10.1016/j.jmbbm.2016.03.005

51. Romano A, Scheel M, Hirsch S, Braun J, Sack I. In vivo waveguide elastography of white matter tracts in the human brain. *Magn Reson Med* 2012; **68**: 1410–22. doi: https://doi.org/10.1002/mrm.24141

52. Tweten DJ, Okamoto RJ, Bayly PV. Requirements for accurate estimation of anisotropic material parameters by magnetic resonance elastography: a computational study. *Magn. Reson. Med.* 2017; **78**: 2360–72. doi: https://doi.org/10.1002/mrm.26600

53. Tweten DJ, Okamoto RJ, Schmidt JL, Garbow JR, Bayly PV. Estimation of material parameters from slow and fast shear waves in an incompressible, transversely isotropic material. *J Biomech* 2015; **48**: 4002–9. doi: https://doi.org/10.1016/j.jbiomech.2015.09.009

54. Schmidt JL, Tweten DJ, Badachhape AA, Reiter AJ, Okamoto RJ, Garbow JR, et al. Measurement of anisotropic mechanical properties in porcine brain white matter ex vivo using magnetic resonance elastography. *J Mech Behav Biomed Mater* 2018; **79**: 30–7. doi: https://doi.org/10.1016/j.jmbbm.2017.11.045

55. Hoover JM, Morris JM, Meyer FB. Use of preoperative magnetic resonance imaging T1 and T2 sequences to determine intraoperative meningioma consistency. *Surg Neurol Int* 2011; **2**: 142. doi: https://doi.org/10.4103/2152-7806.85983

56. Hughes JD, Fattahi N, Van Gompel J, Arani A, Meyer F, Lanzino G, et al. Higher-resolution magnetic resonance elastography in meningiomas to determine intratumoral consistency. *Neurosurgery* 2015; **77**: 653–9. doi: https://doi.org/10.1227/NEU.0000000000000892

57. Murphy MC, Huston J, Glaser KJ, Manduca A, Meyer FB, Lanzino G, et al. Preoperative assessment of meningioma stiffness using magnetic resonance elastography. *J Neurosurg* 2013; **118**: 643–8. doi: https://doi.org/10.3171/2012.9.JNS12519

58. Hughes JD, Fattahi N, Van Gompel J, Arani A, Ehman R, Huston J. Magnetic resonance elastography detects tumoral consistency in pituitary macroadenomas. *Pituitary* 2016; **19**: 286–92. doi: https://doi.org/10.1007/s11102-016-0706-5

59. Sakai N, Takehara Y, Yamashita S, Ohishi N, Kawaji H, Sameshima T, et al. Shear stiffness of 4 common intracranial tumors measured using Mr elastography: comparison with intraoperative consistency grading. *AJNR Am J Neuroradiol* 2016; **37**: 1851–9. doi: https://doi.org/10.3174/ajnr.A4832

60. Yin Z, Glaser KJ, Manduca A, Van Gompel JJ, Link MJ, Hughes JD, et al. Slip interface imaging predicts tumor-brain adhesion in vestibular schwannomas. *Radiology* 2015; **277**: 507–17. doi: https://doi.org/10.1148/radiol.2015151075

61. Yin Z, Hughes JD, Trzasko JD, Glaser KJ, Manduca A, Van Gompel J, Link MJ, et al. Slip interface imaging based on MR-elastography preoperatively predicts meningioma-brain adhesion. *J Magn Reson Imaging* 2017; **46**: 1007–16. doi: https://doi.org/10.1002/jmri.25623

62. Papazoglou S, Xu C, Hamhaber U, Siebert E, Bohner G, Klingebiel R, et al. Scatter-based magnetic resonance elastography. *Phys Med Biol* 2009; **54**: 2229–41. doi: https://doi.org/10.1088/0031-9155/54/7/025

63. Papazoglou S, Hamhaber U, Braun J, Sack I. Horizontal shear wave scattering from a nonwelded interface observed by magnetic resonance elastography. *Phys Med Biol* 2007; **52**: 675–84. doi: https://doi.org/10.1088/0031-9155/52/3/010

64. Streitberger K-J, Reiss-Zimmermann M, Freimann FB, Bayerl S, Guo J, Arlt F, et al. High-resolution mechanical imaging of glioblastoma by multifrequency magnetic resonance elastography. *PLoS One* 2014;

9: e110588. doi: https://doi.org/10.1371/journal.pone.0110588

65. Simon M, Guo J, Papazoglou S, Scholand-Engler H, Erdmann C, Melchert U, et al. Non-Invasive characterization of intracranial tumors by magnetic resonance elastography. *New J Phys* 2013; **15**: 085024. doi: https://doi.org/10.1088/1367-2630/15/8/085024

66. Pepin KM, McGee KP, Arani A, Lake DS, Glaser KJ, Manduca A, et al. MR elastography analysis of glioma stiffness and *IDH1* -mutation status. *AJNR Am J Neuroradiol* 2018; **39**: 31–6. doi: https://doi.org/10.3174/ajnr.A5415

67. Reiss-Zimmermann M, Streitberger K-J, Sack I, Braun J, Arlt F, Fritzsch D, et al. High resolution imaging of viscoelastic properties of intracranial tumours by multi-frequency magnetic resonance elastography. *Clin Neuroradiol* 2015; **25**: 371–8. doi: https://doi.org/10.1007/s00062-014-0311-9

68. Pepin KM, McGee KP. Quantifying tumor stiffness with magnetic resonance elastography: the role of mechanical properties for detection, characterization, and treatment stratification in oncology. *Top Magn Reson Imaging* 2018; **27**: 353–62. doi: https://doi.org/10.1097/RMR.0000000000000181

69. Bunevicius A, Schregel K, Sinkus R, Golby A, Patz S. MR elastography of brain tumors. *Neuroimage Clin* 2020; **25**: 102109. doi: https://doi.org/10.1016/j.nicl.2019.102109

70. Johnson CL, Schwarb H, D.J. McGarry M, Anderson AT, Huesmann GR, Sutton BP, et al. Viscoelasticity of subcortical gray matter structures. *Hum Brain Mapp* 2016; **37**: 4221–33. doi: https://doi.org/10.1002/hbm.23314

71. Huang X, Chafi H, Matthews KL, Carmichael O, Li T, Miao Q, et al. Magnetic resonance elastography of the brain: a study of feasibility and reproducibility using an ergonomic pillow-like passive driver. *Magn Reson Imaging* 2019; **59**: 68–76. doi: https://doi.org/10.1016/j.mri.2019.03.009

72. Sack I, Beierbach B, Wuerfel J, Klatt D, Hamhaber U, Papazoglou S, et al. The impact of aging and gender on brain viscoelasticity. *Neuroimage* 2009; **46**: 652–7. doi: https://doi.org/10.1016/j.neuroimage.2009.02.040

73. Kalra P, Raterman B, Mo X, Kolipaka A. Magnetic resonance elastography of brain: comparison between anisotropic and isotropic stiffness and its correlation to age. *Magn Reson Med* 2019; **82**: 671–9. doi: https://doi.org/10.1002/mrm.27757

74. McIlvain G, Schwarb H, Cohen NJ, Telzer EH, Johnson CL. Mechanical properties of the in vivo adolescent human brain. *Dev Cogn Neurosci* 2018; **34**: 27–33. doi: https://doi.org/10.1016/j.dcn.2018.06.001

75. Wuerfel J, Paul F, Beierbach B, Hamhaber U, Klatt D, Papazoglou S, et al. MR-elastography reveals degradation of tissue integrity in multiple sclerosis. *Neuroimage* 2010; **49**: 2520–5. doi: https://doi.org/10.1016/j.neuroimage.2009.06.018

76. Sack I, Streitberger K-J, Krefting D, Paul F, Braun J. The influence of physiological aging and atrophy on brain viscoelastic properties in humans. *PLoS One* 2011; **6**: e23451. doi: https://doi.org/10.1371/journal.pone.0023451

77. Zhang J, Green MA, Sinkus R, Bilston LE. Viscoelastic properties of human cerebellum using magnetic resonance elastography. *J Biomech* 2011; **44**: 1909–13. doi: https://doi.org/10.1016/j.jbiomech.2011.04.034

78. McCracken PJ, Manduca A, Felmlee J, Ehman RL. Mechanical transient-based magnetic resonance elastography. *Magn Reson Med* 2005; **53**: 628–39. doi: https://doi.org/10.1002/mrm.20388

79. Clayton EH, Genin GM, Bayly PV, Transmission BPV. Transmission, attenuation and reflection of shear waves in the human brain. *J R Soc Interface* 2012; **9**: 2899–910. doi: https://doi.org/10.1098/rsif.2012.0325

80. Braun J, Guo J, Lützkendorf R, Stadler J, Papazoglou S, Hirsch S, et al. High-Resolution mechanical imaging of the human brain by three-dimensional multifrequency magnetic resonance elastography at 7T. *Neuroimage* 2014; **90**: 308–14. doi: https://doi.org/10.1016/j.neuroimage.2013.12.032

81. Kruse SA, Rose GH, Glaser KJ, Manduca A, Felmlee JP, Jack CR, et al. Magnetic resonance elastography of the brain. *Neuroimage* 2008; **39**: 231–7. doi: https://doi.org/10.1016/j.neuroimage.2007.08.030

82. Hiscox LV, McGarry MDJ, Schwarb H, Van Houten EEW, Pohlig RT, Roberts N, et al. Standard-space atlas of the viscoelastic properties of the human brain. *Hum Brain Mapp* 2020; **41**: 5282: 5300. doi: https://doi.org/10.1002/hbm.25192

83. Streitberger K-J, Sack I, Krefting D, Pfüller C, Braun J, Paul F, et al. Brain viscoelasticity alteration in chronic-progressive multiple sclerosis. *PLoS One* 2012; **7**: e29888. doi: https://doi.org/10.1371/journal.pone.0029888

84. Murphy MC, Huston J, Jack CR, Glaser KJ, Manduca A, Felmlee JP, et al. Decreased brain stiffness in Alzheimer's disease determined by magnetic resonance elastography. *J Magn Reson Imaging* 2011;

34: 494–8. doi: https://doi.org/10.1002/jmri.22707

85. ElSheikh M, Arani A, Perry A, Boeve BF, Meyer FB, Savica R, et al. MR elastography demonstrates unique regional brain stiffness patterns in dementias. *AJR Am J Roentgenol* 2017; **209**: 403–8. doi: https://doi.org/10.2214/AJR.16.17455

86. Lipp A, Skowronek C, Fehlner A, Streitberger K-J, Braun J, Sack I. Progressive supranuclear palsy and idiopathic Parkinson's disease are associated with local reduction of in vivo brain viscoelasticity. *Eur Radiol* 2018; **28**: 3347–54. doi: https://doi.org/10.1007/s00330-017-5269-y

87. Arani A, Min H-K, Fattahi N, Wetjen NM, Trzasko JD, Manduca A, et al. Acute pressure changes in the brain are correlated with Mr elastography stiffness measurements: initial feasibility in an in vivo large animal model. *Magn Reson Med* 2018; **79**: 1043–51. doi: https://doi.org/10.1002/mrm.26738

88. Hatt A, Cheng S, Tan K, Sinkus R, Bilston LE. Mr elastography can be used to measure brain stiffness changes as a result of altered cranial venous drainage during jugular compression. *AJNR Am J Neuroradiol* 2015; **36**: 1971–7. doi: https://doi.org/10.3174/ajnr.A4361

89. Hetzer S, Dittmann F, Bormann K, Hirsch S, Lipp A, Wang DJJ, et al. Hypercapnia increases brain viscoelasticity. *J Cereb Blood Flow Metab* 2019; **39**: 2445–55. doi: https://doi.org/10.1177/0271678X18799241

90. Hetzer S, Birr P, Fehlner A, Hirsch S, Dittmann F, Barnhill E, et al. Perfusion alters stiffness of deep gray matter. *J Cereb Blood Flow Metab* 2018; **38**: 116–25. doi: https://doi.org/10.1177/0271678X17691530

91. Kolipaka A, Wassenaar PA, Cha S, Marashdeh WM, Mo X, Kalra P, et al. Magnetic resonance elastography to estimate brain stiffness: measurement reproducibility and its estimate in pseudotumor cerebri patients. *Clin Imaging* 2018; **51**: 114–22. doi: https://doi.org/10.1016/j.clinimag.2018.02.005

92. Streitberger K-J, Wiener E, Hoffmann J, Freimann FB, Klatt D, Braun J, et al. In vivo viscoelastic properties of the brain in normal pressure hydrocephalus. *NMR Biomed* 2011; **24**: 385–92. doi: https://doi.org/10.1002/nbm.1602

93. Freimann FB, Streitberger K-J, Klatt D, Lin K, McLaughlin J, Braun J, et al. Alteration of brain viscoelasticity after shunt treatment in normal pressure hydrocephalus. *Neuroradiology* 2012; **54**: 189–96. doi: https://doi.org/10.1007/s00234-011-0871-1

94. Fattahi N, Arani A, Perry A, Meyer F, Manduca A, Glaser K, et al. Mr elastography demonstrates increased brain stiffness in normal pressure hydrocephalus. *AJNR Am J Neuroradiol* 2016; **37**: 462–7. doi: https://doi.org/10.3174/ajnr.A4560

95. Perry A, Graffeo CS, Fattahi N, ElSheikh MM, Cray N, Arani A, et al. Clinical correlation of abnormal findings on magnetic resonance elastography in idiopathic normal pressure hydrocephalus. *World Neurosurg* 2017; **99**: 695–700. doi: https://doi.org/10.1016/j.wneu.2016.12.121

96. Fattahi N, Arani A, Perry A, Meyer F, Manduca A, Glaser K, et al. Mr elastography demonstrates increased brain stiffness in normal pressure hydrocephalus. *AJNR Am J Neuroradiol* 2016; **37**(S1): 462–7. doi: https://doi.org/10.3174/ajnr.A4560

97. Murphy MC, Cogswell PM, Trzasko JD, Manduca A, Senjem ML, Meyer FB, et al. Identification of normal pressure hydrocephalus by disease-specific patterns of brain stiffness and damping ratio. *Invest Radiol* 2020; **55**: 200: 208. doi: https://doi.org/10.1097/RLI.0000000000000630

98. Schwarb H, Johnson CL, McGarry MDJ, Cohen NJ. Medial temporal lobe viscoelasticity and relational memory performance. *Neuroimage* 2016; **132**: 534–41. doi: https://doi.org/10.1016/j.neuroimage.2016.02.059

99. Schwarb H, Johnson CL, Daugherty AM, Hillman CH, Kramer AF, Cohen NJ, et al. Aerobic fitness, hippocampal viscoelasticity, and relational memory performance. *Neuroimage* 2017; **153**: 179–88. doi: https://doi.org/10.1016/j.neuroimage.2017.03.061

100. Hiscox LV, Johnson CL, McGarry MDJ, Schwarb H, van Beek EJR, Roberts N, et al. Hippocampal viscoelasticity and episodic memory performance in healthy older adults examined with magnetic resonance elastography. *Brain Imaging Behav* 2020; **14**: 175–85. doi: https://doi.org/10.1007/s11682-018-9988-8

101. Sandroff BM, Johnson CL, Motl RW. Exercise training effects on memory and hippocampal viscoelasticity in multiple sclerosis: a novel application of magnetic resonance elastography. *Neuroradiology* 2017; **59**: 61–7. doi: https://doi.org/10.1007/s00234-016-1767-x

102. Fehlner A, Hirsch S, Guo J, Braun J, Sack I. The viscoelastic response of the human brain to functional activation detected by magnetic resonance elastography. *Proc Intl Soc Mag Reson Med* 2014; **22**: 871.

103. Patz S, Nazari N, Earborne P. Functional neuroimaging in the brain using magnetic resonance elastography. *Proc Intl Soc Mag Reson Med* 2017; **25**: 242.

104. Patz S, Fovargue D, Schregel K, Nazari N, Palotai M, Barbone PE, et al. Imaging localized neuronal activity at fast time scales through biomechanics. *Sci Adv* 2019; **5**: eaav3816. doi: https://doi.org/10.1126/sciadv.aav3816

105. de Arcos J, Fovargue D, Schregel K, Neji R, Patz S, Sinkus R. Imaging primary neuronal activity in the human optical cortex at 1.35 Hz. *In Soc Magn Reson Med* 2018; **2018**: 147.

106. Lan PS, Glaser KJ, Ehman RL, Glover GH. Imaging brain function with simultaneous BOLD and viscoelasticity contrast: fMRI/fMRE. *Neuroimage* 2020; **211**: 116592. doi: https://doi.org/10.1016/j.neuroimage.2020.116592

107. Moeskops P, Viergever MA, Mendrik AM, de Vries LS, Benders MJNL, Išgum I. Automatic segmentation of Mr brain images with a convolutional neural network. *IEEE Trans Med Imaging* 2016; **35**: 1252–61. doi: https://doi.org/10.1109/TMI.2016.2548501

108. Fedorov A, Damaraju E, Calhoun V, Plis S. Almost instant brain atlas segmentation for large-scale studies. *arXiv* 2017; **17**: 44.

109. Murphy MC, Manduca A, Trzasko JD, Glaser KJ, Huston J, Ehman RL. Artificial neural networks for stiffness estimation in magnetic resonance elastography. *Magn Reson Med* 2018; **80**: 351–60. doi: https://doi.org/10.1002/mrm.27019

110. Solamen L, Shi Y, Amoh J. Dual objective approach using a Convolutional neural network for magnetic resonance elastography. *arXiv preprint arXiv* 2018; **181200441**.

111. Scott JM, Arani A, Manduca A, McGee KP, Trzasko JD, Huston J, et al. Artificial neural networks for magnetic resonance elastography stiffness estimation in inhomogeneous materials. *Med Image Anal* 2020; **63**: 101710. doi: https://doi.org/10.1016/j.media.2020.101710

112. Holm S. Spring-damper equivalents of the fractional, poroelastic, and poroviscoelastic models for elastography. *NMR Biomed* 2018; **31**: e3854. doi: https://doi.org/10.1002/nbm.3854

113. Phillip RP, Steven PM, Francis EK. 3D finite element solution to the dynamic poroelasticity problem for use in MR elastography. *Proc Intl Soc Mag Reson Med* 2007; **6511**: 65111B.